JOURNAL OF MATERIALS SCIENCE **34** (1999) 2169–2173

Effect of Sr-doping on the structural and electrical properties of gadolinium manganite oxide

G. CH. KOSTOGLOUDIS, CH. FTIKOS
Laboratory of Inorganic Materials Technology, Department of Chemical Engineering, National Technical University of Athens, 9 Heroon Polytechniou Str., Zografou Campus, GR-157 80 Athens, Greece
E-mail: gkostog@central.ntua.gr

The crystal structure and electrical conductivity of the perovskite oxide system $Gd_{1-x}Sr_xMnO_{3\pm\delta}$ ($x = 0$–0.5) were investigated. The effect of the level of Sr-doping on these properties was examined. An orthorhombic $GdFeO_3$-type structure (space group Pbnm) was found for all oxides. The room temperature lattice parameters were determined from the XRD data. A large distortion of the unit cell was observed in the case of the undoped compound. The distortion was gradually reduced with increasing Sr content. The unit cell volume decreased on Sr-doping. The electrical conductivity of the oxides was measured from room temperature up to 800 °C. The small polaron hopping conductivity model can adequately describe the electrical conductivity behavior. The activation energy decreases as x increases.

1. Introduction

Rare earth manganite perovskite oxides have attracted much attention in recent years due to their incorporation as cathodes in Solid Oxide Fuel Cells (SOFCs) [1]. The compositions with La at the A-site have been extensively investigated [2, 3], while less attention has been given to other rare earth manganites. The purpose of the present investigation was to study the crystallographic and electrical conductivity properties of the oxides in the system $Gd_{1-x}Sr_xMnO_{3\pm\delta}$ ($x = 0$–0.5). The effect of the level of Sr-doping on these properties was examined.

2. Experimental procedure

Ceramic powders of the composition $Gd_{1-x}Sr_xMnO_{3\pm\delta}$ ($x = 0$–0.5) were prepared by the citrate synthesis and pyrolysis method [4]. The powder was calcined in air at 1200 °C for 15 h, and then wet milled with acetone in a satellite-type milling apparatus using zirconia balls. After drying, the powders were compacted by cold isostatic pressing (250 MPa) in the shape of cylindrical rods of approximate dimensions 50 mm length and 6 mm diameter. The compacts were then sintered in air at 1400 °C for 15 h, with a heating and cooling rate of 1 °C/min. The bulk densities of the sintered samples were measured by the Archimedes' method. In all cases densities above 92% of the theoretical values were obtained.

The structural study was performed on the calcined oxide powders, at room temperature, by X-ray powder diffraction (XRD). A SIEMENS D5000 diffractometer (CuK_α radiation) was used, operated at 40 kV and 30 mA. The XRD data were collected by step scanning in the range $10 \leq 2\theta \leq 80$ in increments of 0.02° 2θ. The lattice parameters were determined using a least squares unit cell refinement computer program (LSUCR). The electrical conductivity was measured on the sintered rods in air by the standard four-point DC method, upon heating in the temperature range 100–800 °C at a heating rate of 5 °C/min. At each temperature at which measurement was taken the sample remained for 20 min, so that equilibrium was established.

3. Results and discussion

3.1. Crystal structure

The X-ray powder diffraction patterns of the oxides in the system $Gd_{1-x}Sr_xMnO_{3\pm\delta}$ ($x = 0$–0.5) are shown in Fig. 1. In the case of the Sr-free compound the peak splitting is large, indicating a severe distortion from the ideal cubic perovskite structure. As the Sr content increases, the peak splitting is gradually reduced, and it is not visible for $x \geq 0.4$. In all cases, the patterns were indexed in the orthorhombic Pbnm space group ($GdFeO_3$-type structure [5]). Each unit cell consists of four units, and has the approximate dimensions $(2)^{1/2}\,a_p \times (2)^{1/2}\,a_p \times 2a_p$, where a_p is the lattice parameter of the ideal cubic unit cell. The determined lattice parameters of the orthorhombic cell are shown in Table I, and also drawn in Fig. 2 as a function of Sr content. As can be seen, there is a large deviation among the parameters a, b and $c/(2)^{1/2}$ of the Sr-free compound, while as x increases, the deviation is reduced, and for $x = 0.5$ the values of the parameters are almost equal. The relation among the lattice parameters, a, b and $c/(2)^{1/2}$, can provide a measure of the distortion of the unit cell. This relation is included in

TABLE I Phase symmetry, lattice parameters, unit cell volume, orthorhombic deformation D (%), and type of orthorhombic structure of the system $Gd_{1-x}Sr_xMnO_{3\pm\delta}$

x(mol)	Phase symmetry	a(Å)	b(Å)	c(Å)	Volume (Å^3)	$c/(2)^{1/2}$ (Å)	$a, b, c/(2)^{1/2}$ relation	Orthorhombic deformation D (%)	Type of orthorhombic structure
0	Orthorhombic	5.3942	5.6716	7.4283	227.3	5.2526	$c/\sqrt{2} < a < b$	2.83	O′-type
0.15	Orthorhombic	5.3517	5.5884	7.5222	225.0	5.3190	$c/\sqrt{2} < a < b$	2.07	O′-type
0.3	Orthorhombic	5.3913	5.4730	7.5906	224.0	5.3674	$c/\sqrt{2} < a < b$	0.77	O′-type
0.4	Orthorhombic	5.3998	5.4315	7.6314	223.8	5.3962	$c/\sqrt{2} \approx a < b$	0.28	O-type
0.5	Orthorhombic	5.4041	5.4132	7.6482	223.7	5.4081	$a < c/\sqrt{2} < b$	0.06	O-type

Table I. Generally, two types of orthorhombic structures are distinguished. The O-type structure, which is characterized by the relationship $a \leq c/(2)^{1/2} \leq b$, exists when the lattice deformation is relatively small, while the O′-type structure, with $c/(2)^{1/2} \leq a \leq b$, exists in the case of enhanced lattice deformation. The structure of $Gd_{1-x}Sr_xMnO_{3\pm\delta}$ is O′-type for $x = 0$, 0.15 and 0.3, and O-type for $x = 0.4$ and 0.5.

In order to quantitatively express the macroscopic distortion relative to the ideal perovskite structure, the quantity D (% orthorhombic deformation) is defined as [6]:

$$D = \frac{1}{3}\sum_{i=1}^{3}\left|\frac{\alpha_i - \bar{\alpha}}{\bar{\alpha}}\right| \times 100 \qquad (1)$$

where $a_1 = a$, $a_2 = b$, $a_3 = c/(2)^{1/2}$, and $\bar{\alpha} = (abc/(2)^{1/2})^{1/3}$. The values of D, calculated from Equation 1, are illustrated in Fig. 3. D is large in the case of the undoped compound, and it decreases as Sr doping increases. For $x = 0.5$, D is almost zero. In Fig. 3, the values of the Goldschmidt [7] tolerance factor, t, are also shown. The tolerance factor expresses the bond-length

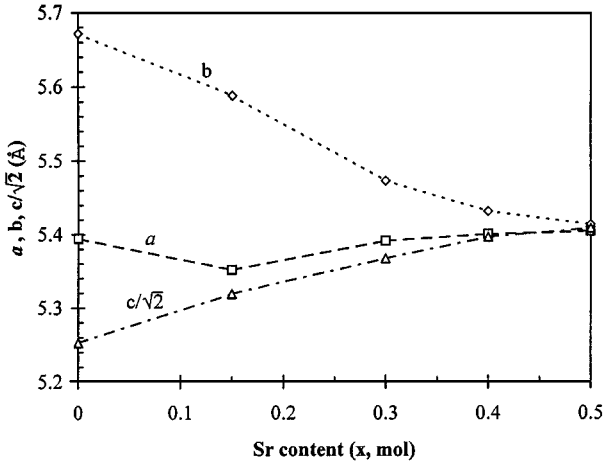

Figure 2 Room temperature lattice parameters of $Gd_{1-x}Sr_xMnO_{3\pm\delta}$ as a function of Sr content (x, mol).

mismatch in an ABO_3 perovskite, and it is given by the following equation:

$$t = \frac{r_A + r_O}{(2)^{1/2}(r_B + r_O)} \qquad (2)$$

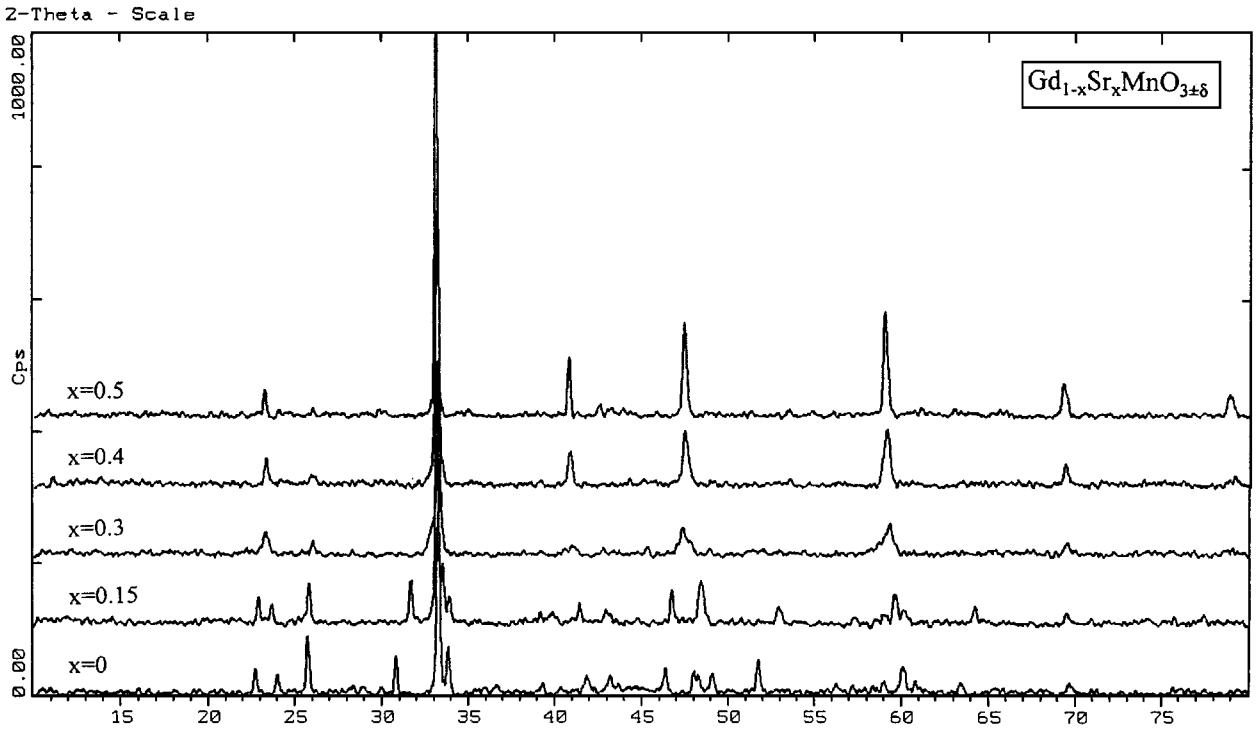

Figure 1 X-ray powder diffraction patterns of $Gd_{1-x}Sr_xMnO_{3\pm\delta}$.

TABLE II Ionic radii of several ions, and their coordination number (CN) in the perovskite lattice [8]

Cation	Ionic radius (Å)
Gd^{3+} (CN = 12)	1.21
Sr^{2+} (CN = 12)	1.44
Mn^{3+} (CN = 6)	0.645
Mn^{4+} (CN = 6)	0.530
O^{2-} (CN = 6)	1.40

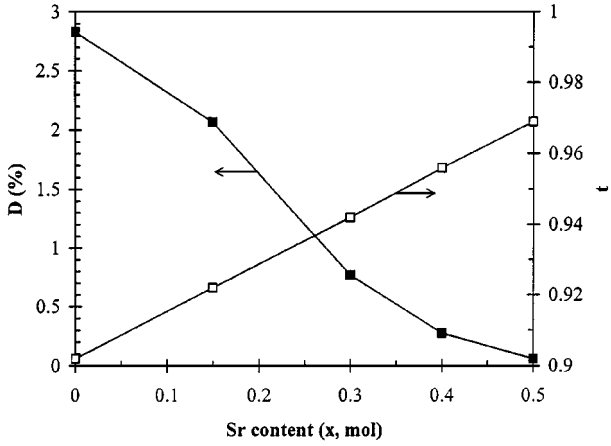

Figure 3 Orthorhombic deformation (D, %) and tolerance factor (t) of $Gd_{1-x}Sr_xMnO_{3\pm\delta}$ as a function of Sr content (x, mol).

The values of t were calculated using Shannon's [8] ionic radii (Table II). For the Sr-doped manganites, where both Gd^{3+} and Sr^{2+} cations occupy the A-site, the tolerance factors were calculated from the weighted average radii of these cations. A $t < 1$ is obtained in all cases. The tolerance factor comes closer to unity as Sr content increases. If cations A^{3+} and B^{3+} could be found such that $t = 1$, the ideal cubic perovskite structure would be formed. In the case of the gadolinium manganite oxide, however, a $t < 1$ is accommodated by a cooperative rotation of the MnO_6 octahedra about the (110) axis to give the orthorhombic Pbnm structure. This is caused by the small size of the Gd^{3+} cation, which is located at the center of the unit cell. As Sr^{2+} is substituted for Gd^{3+}, a net increase of the size of the A-site cation occurs, due to the larger Sr^{2+} cation compared to Gd^{3+} (Table II). Moreover, the incorporation of the lower valence Sr^{2+} cations in Gd^{3+} lattice positions results in the oxidation of Mn^{3+} cations to Mn^{4+} for charge compensation reasons:

$$SrMnO_3 \xrightarrow[GdMnO_3]{} Sr'_{Gd} + Mn^{\cdot}_{Mn} + 3O^{\times}_{O} \qquad (3)$$

where Kröger-Vink notation [9] is used. The smaller size of Mn^{4+} cation compared to Mn^{3+}, causes the net decrease of the B-site cation. The increase of r_A and decrease of r_B, owing to the increase of Sr content, result in the increase of the tolerance factor (Equation 2). As t comes closer to unity, D decreases, and the deviation among the lattice parameters also decreases.

To illustrate the effect of Sr doping on the size of the unit cell, the pseudo-cubic lattice constant (a') is

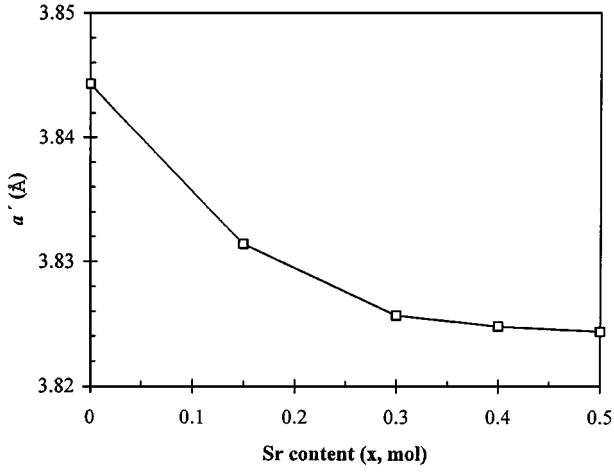

Figure 4 Pseudo-cubic lattice constant (a') of $Gd_{1-x}Sr_xMnO_{3\pm\delta}$ as a function of x.

defined as the cube root of the unit cell volume per ABO_3 unit:

$$a' = (V/z)^{1/3} \qquad (4)$$

where $z = 4$ for the oxides of this study. The values of a' are drawn in Fig. 4, as a function of Sr content. As can be seen, a' decreases as x increases. Considering the radii of the ions involved (Table II), it can be seen that the relative decrease of a' due to Mn oxidation is greater than its relative increase due to Sr^{2+} substitution. Therefore, a net decrease in the size of a' results when x increases in $Gd_{1-x}Sr_xMnO_{3\pm\delta}$. In addition, according to Pauling's second rule, concerning bond strength [10], the formation of the tetravalent Mn ions is expected to strengthen the Mn-O bonds in MnO_6 octahedra. As a result, the size of MnO_6 octahedra and the volume of the perovskite unit cell decrease.

3.2. Electrical conductivity

The logarithm of electrical conductivity ($\log\sigma$) of $Gd_{1-x}Sr_xMnO_{3\pm\delta}$ ($x = 0$–0.5) is shown in Fig. 5 as a function of reciprocal temperature ($1000/T$). The conductivity increases with temperature for all compositions (semiconducting electrical behavior). In Fig. 6 it can be seen that there is a linear relationship between $\log\sigma T$ and $1/T$, indicating that the conduction may be explained by the small polaron hopping mechanism. The Mn^{4+} cations can be considered as p-type small polarons (holes). In the undoped compound, Mn^{4+} cations exist at $pO_2 = 0.21$, due to the appearance of oxygen excess and cation vacancies [11–13], according to the defect reaction:

$$6Mn^{\times}_{Mn} + \frac{3}{2}O_2 \Leftrightarrow V'''_{Gd} + V'''_{Mn} + 6Mn^{\cdot}_{Mn} + 3O^{\times}_{O} \qquad (5)$$

In the Sr-doped compounds, Mn^{4+} cations are formed by Equation 3. The small polaron is formed by the difference in ionic radii between Mn^{4+} and Mn^{3+} cations, which produces a local distortion that can trap the charge at Mn^{4+} lattice positions. Provided that sufficient energy is acquired, the polaron can hop among Mn

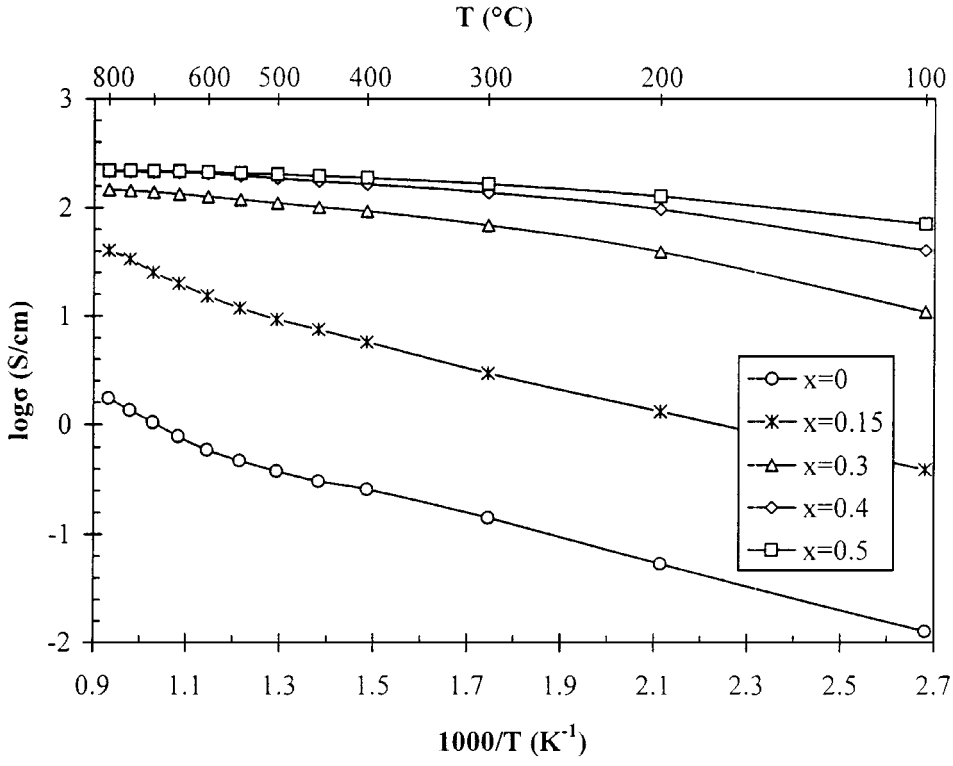

Figure 5 Logarithm of electrical conductivity ($\log\sigma$) versus reciprocal temperature ($1000/T$) for $Gd_{1-x}Sr_xMnO_{3\pm\delta}$ in air.

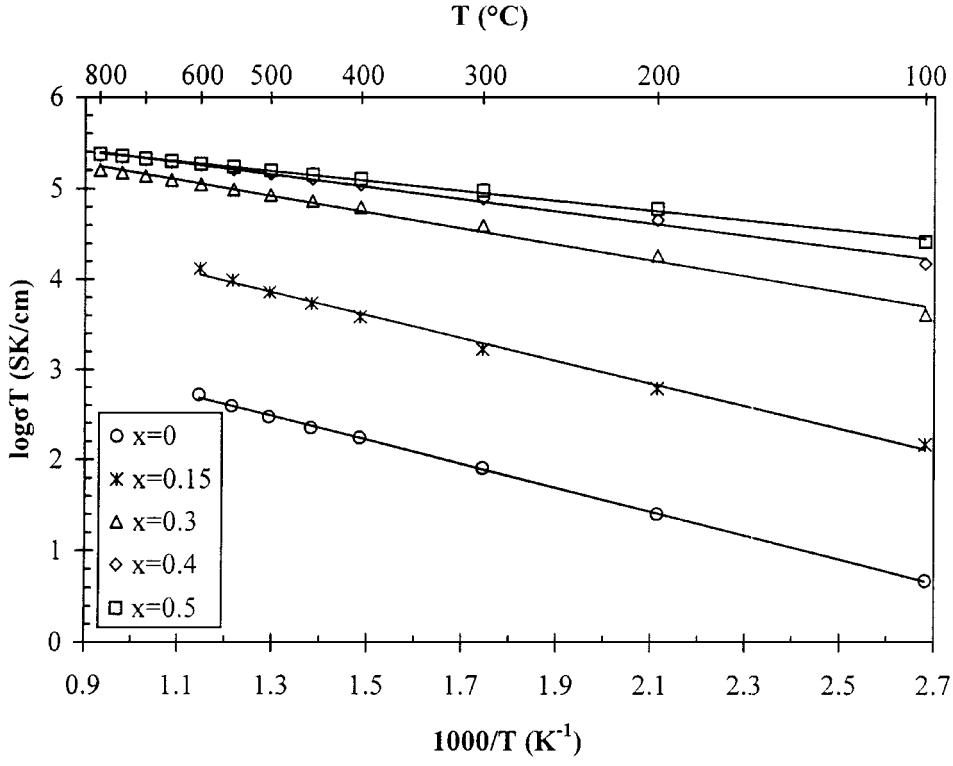

Figure 6 $\mathrm{Log}\,\sigma T$ vs. $1000/T$ plots for $Gd_{1-x}Sr_xMnO_{3\pm\delta}$ in air.

sites. Thus, when the temperature is raised, the mobility of small polarons is increased, resulting in the observed conductivity increase.

The dependence of electrical conductivity on Sr content (x) is clarified in Fig. 7. The conductivity increases constantly with x for all examined temperatures. The reason for this behavior is the concurrent increase of the charge carriers (Mn^{4+}), produced according to Equation 3. A higher concentration of charge carriers results to higher conductivity values.

The temperature dependence of electrical conductivity through the small polaron hopping mechanism is express by:

$$\sigma = \frac{A}{T}\exp(-E_a/kT) \qquad (6)$$

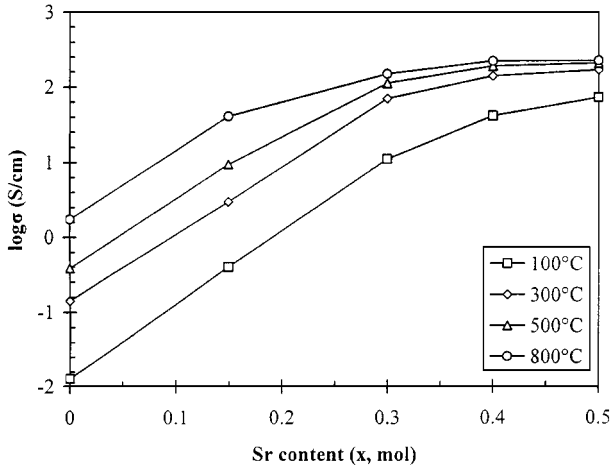

Figure 7 Log σ vs. Sr content (x, mol) for $Gd_{1-x}Sr_xMnO_{3\pm\delta}$.

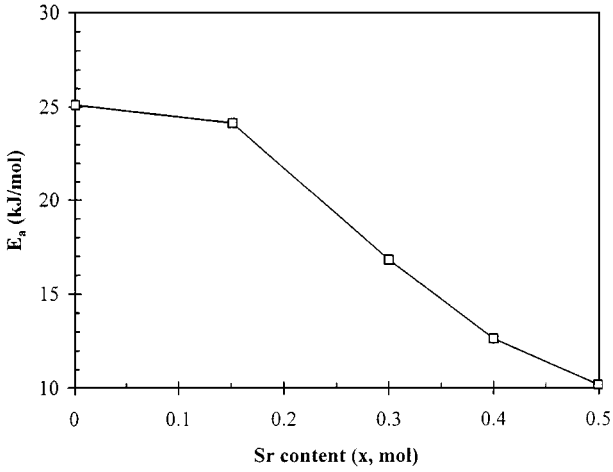

Figure 8 Activation energy (E_a) for small polaron hopping conduction in the system $Gd_{1-x}Sr_xMnO_{3\pm\delta}$ as a function of Sr content (x, mol).

in which E_a is the activation energy for hopping, k is the Boltzmann constant, T is the absolute temperature and A is the pre-exponential factor. The $\log \sigma T$ vs. $1/T$ plot should give a straight line, from the slope of which, the activation energy can be calculated. The E_a values of the $Gd_{1-x}Sr_xMnO_{3\pm\delta}$ oxides, calculated from the slopes of the lines of Fig. 6, are shown in Fig. 8. The activation energies range from 25.1 kJ/mol for the undoped compound, to 10.2 kJ/mol for the composition with 50 mol % Sr, and they are compatible with those observed for other rare earth manganites [14–16]. The low activation energies are in agreement with the small polaron hopping conduction mechanism. As can be seen in Fig. 8, E_a decreases with increasing Sr content. The larger size of the Sr^{2+} cations compared to Gd^{3+}, and in addition the smaller Mn^{4+} cations (formed by Equation 3) compared to Mn^{3+}, brings the Mn-O-Mn angle closer to 180°. As a result, the orbital overlap between adjacent ions is increased. Thus, the interaction integral β is increased, which is proportional to the width of the Mn-O bands [17]. The increase of the bandwidth results in the observed decrease of the activation energy.

4. Conclusions

The oxides in the system $Gd_{1-x}Sr_xMnO_{3\pm\delta}$ (x = 0–0.5) were found to have an orthorhombic $GdFeO_3$-type perovskite structure (space group Pbnm). The Sr-free compound is severely distorted, but this distortion is gradually reduced, as the level of Sr-doping is increased. The pseudo-cubic lattice constant decreases with increasing Sr content, due to the oxidation of the Mn^{3+} cations to the smaller Mn^{4+} cations. The electrical conductivity behavior of the oxides is temperature activated (semiconducting-type), and can be described by the small polaron hopping conductivity model. Higher conductivities are achieved by compositions with higher level of Sr content as a result of the increase in the concentration of charge carriers (Mn^{4+}). Low values of activation energy were calculated, in agreement with the small polaron hopping conductivity model. The activation energy decreases with increasing Sr content.

References

1. N. Q. MINH, *J. Amer. Ceram. Soc.* **76** (1993) 563.
2. J. A. M. VAN ROOSMALEN, J. P. P. HUIJSMANS and L. PLOMP *Solid State Ionics* **66** (1993) 279.
3. A. HAMMOUCHE, E. SIEBERT and A. HAMMOU, *Mater. Res. Bull.* **24** (1989) 367.
4. D. H. A. BLANK, H. KRUIDHOF and J. FLOKSTRA, *J. Phys. D***21** (1988) 226.
5. S. GELLER, *J. Chem. Phys.* **24** (1656) 1236.
6. K. KNIZEK, Z. JIRAK, E. POLLERT and F. ZOUNOVA, *J. Solid State Chem.* **100** (1992) 292.
7. V. M. GOLDSCHMIDT, Skrifter Norske Videnskaps-Akad. Oslo. I. Mathemat. Naturwiss. Klasse No. **8** (1926).
8. R. D. SHANNON, *Acta Crystallogr.* **A32** (1976) 751.
9. F. A. KRÖGER and V. J. VINK, in "Solid State Physics," Vol. 3, edited by F. Seitz and D. Turnbull (Academic Press, New York, 1956) p. 307.
10. L. PAULING, "The Nature of the Chemical Bond," 3rd ed. (Cornell University Press, Ithaca, NY, 1960) p. 547.
11. J. H. KUO, H. U. ANDERSON and D. M. SPARLIN, *J. Solid State Chem.* **83** (1989) 52.
12. J. A. M. VAN ROOSMALEN, E. H. P. CORDFUNKE, R. B. HELMOLDT and H. W. ZANDBERGEN, *ibid.* **110** (1994) 100.
13. V. A. CHEREPANOV, L. YU. BURKHATOVA, A. N. PETROV and V. I. VORONIN, *ibid.* **118** (1995) 53.
14. G. CH. KOSTOGLOUDIS, N. VASILAKOS and CH. FTIKOS, *J. Eur. Ceram. Soc.* **17** (1997) 1513.
15. G. CH. KOSTOGLOUDIS and CH. FTIKOS, *ibid.* in press.
16. P. SHUK, L. TICHONOVA and U. GUTH, *Solid State Ionics* **68** (1994) 177.
17. J. K. BURDETT, "Chemical Bonding in Solids" (Oxford University Press, Oxford, 1995) p. 167.

Received 23 December 1997
and accepted 26 October 1998